CSIAM Trans. Life Sci.
doi: 10.4208/csiam-ls.SO-2025-0002

Vol. **x**, No. x, pp. 1-30
xx 2025

Invasion Dynamics of Alien Mussels: A Mussel-Algae Model with Time Delay in Filter Feeding and Environmental Variability

Wenxu Ning[1], Jie Lou[2], Litao Han[3] and Sanling Yuan[1,*]

[1] *College of Science, University of Shanghai for Science and Technology, Shanghai 200093, P.R. China.*
[2] *Department of Mathematics, Shanghai University, Shanghai 200444, P.R. China.*
[3] *School of Mathematics, Renmin University of China, Beijing 100872, P.R. China.*

Received 3 March 2025; Accepted 6 July 2025

Abstract. The dynamic behavior of alien mussels interacting with algae after arriving in a new environment has long been a focus of invasion ecology research. This paper extends and analyzes a classical mussel-algae model by incorporating a time delay in mussel filter feeding and accounting for environmental variability. We theoretically study the stochastic dynamics, including the global existence and uniqueness of the positive solution, the existence of a unique stationary distribution, and mussel extinction, using tools from stochastic analysis. Furthermore, we derive an explicit expression for the probability density function around the quasi-stable equilibrium by solving the corresponding Fokker-Planck equation. Our theoretical and numerical results indicate that: (a) larger environmental disturbances or artificial removal can effectively prevent the survival of alien mussels in novel habitats, (b) a decreased filter feeding rate leads to an accelerated extinction rate of mussels, and (c) an increased consumption constant c decelerates the transition rate of mussels from the initial state to the extinction state, as analyzed through the mean first passage time of mussels. These findings highlight the complex interaction between intrinsic and extrinsic factors in influencing the invasion dynamics of alien mussels.

AMS subject classifications: 34F05, 92B05, 37H10
Key words: Stochastic mussel-algae model, infinite distributed delay, stationary distribution, extinction, density function.

1 Introduction

Globally, biological invasions pose a significant threat to biodiversity and ecosystem function [38]. Invasive species impact ecosystems through competitive interactions, predation on native species, habitat alterations, nutrient cycles, and energy budgets [2, 21].

*Corresponding author. *Email address:* sanling@usst.edu.cn (S. L. Yuan),

The zebra mussel exemplifies a highly successful invasive species, distinguished by its prolific reproductive capacity, rapid growth rate, broad tolerance to diverse physical and chemical conditions, and its ability to establish advantageous interactions with native species [26]. One major consequence of zebra mussels invasion is biofouling, which obstructs water intake structures, such as pipes and screens, thereby impairing pumping efficiency for power and water treatment facilities, and incurring costs for industries, businesses, and communities. In addition, recreation-based industries and activities have also been significantly affected, as docks, buoys, boats, and beaches have been extensively colonized [25].

Zebra mussels also disrupt the ecosystems they invade. They can shift lakes from a turbid, phytoplankton-dominated state to a clear, macrophyte-dominated state through filter-feeding, potentially leading to increased competition, decreased survival, and reduced biomass of planktivorous fish [9, 31]. After filter-feeding, the mussels release unwanted inorganic particles as pseudofeces. The decomposition of this waste consumes oxygen, lowers pH, and produces toxic byproducts. Additionally, biomagnification of organic pollutants can occur as pseudofeces are passed up the food chain [3].

Control and prevention of macrofouling caused by zebra mussels have become major concerns for managers of various water delivery systems. Currently, there are several management techniques to control invasive mussels, including mechanical removal [35], oxidizing biocides [42], and biological control [37]. The ineffectiveness of traditional control strategies and their potential environmental harm necessitate a shift toward prevention as the optimal approach for managing invasive species [1]. Consequently, a thorough investigation into the population dynamics of zebra mussels can enhance our understanding of their invasion conditions. Moreover, manual counting remains the primary method for quantifying the population size of benthic fauna [6], which poses challenges due to the potential magnitude of the population. In this context, some mathematical models yield interesting quantitative results [39]. Additionally, a mathematical model can provide qualitative insights into infestation dynamics, effectively aiding in the prevention process. Thus, a model considering the interaction of mussels and algae could be beneficial for evaluating invasion potential and population control strategies [15, 24].

Recent research modeling the interaction between algae and mussels has been conducted in [1, 4, 15, 18, 19, 32, 34]. Koppel *et al.* [15], first proposed a mathematical model of algae and mussels based on a distinct mechanism: reduced mussel mortality at high mussel density, leading to intraspecific facilitation. Their study emphasizes that self-organization may influence resource flow through ecosystems, thereby affecting ecosystem functioning at larger spatial scales. Cangelosi *et al.* [4] extended the model in [15] by substituting the advective term in the algae equation with a lateral diffusive term for mussel biomass density and algae concentration in a quiescent marine layer over an unbounded soft sedimentary substrate, predicting periodic mussel bed patterns in this context. Silva *et al.* [32] developed a three-dimensional mathematical model incorporating the relationships among larvae, mussels, and algae, integrating hydrodynamics and population dynamics. They quantified the population of the invasive golden mussel in

hydroelectric power plant reservoirs by integrating field observation data with computational simulations. Following the work of Silva *et al.* [32], Barbosa *et al.* [1] analyzed potential infestation scenarios in a particular case of the diffusion-convection model by examining the stability of its equilibrium points while disregarding spatial terms, diffusion, and transport. In this paper, inspired by Barbosa *et al.* [1], we omit advection due to tidal currents and mussel diffusion from [15], instead introducing manual removal of invasive mussels via a linear term, $EM(t)$, where E represents the removal rates applied to the mussel species. Here is our deterministic model of mussel-algae interaction incorporating mussel removal

$$\begin{cases} \dfrac{\mathrm{d}A(t)}{\mathrm{d}t} = \big(A_{up} - A(t)\big)f - \dfrac{c}{h}A(t)M(t), \\ \dfrac{\mathrm{d}M(t)}{\mathrm{d}t} = e_1 cM(t)A(t) - \dfrac{dkM(t)}{k+M(t)} - EM(t), \end{cases} \tag{1.1}$$

where $A(t)$ denotes the algal concentration in the benthic boundary layer and $M(t)$ represents the density of mussels. Key parameters include A_{up} (the concentration of algae in the surface layer), f (the rate of exchange between the lower and upper water layers), c (the consumption constant), h (the height of the lower water layer), e_1 (the conversion constant of ingested algae to mussel biomass), d (the maximal per capita mussel mortality rate), and k (the saturation rate of mussels). The term $dkM(t)/(k+M(t))$ indicates that the per capita mortality of mussels is assumed to decrease with increasing mussel density due to reduced dislodgment and predation in dense aggregations.

The destruction of invaded ecosystems by mussels is primarily attributed to their filter-feeding behavior, wherein water is ingested through an inhalant siphon, leaving behind required algae after a period of filtration, and expelling unwanted particles as pseudofeces [16]. Given that water temperature, particle type, size, and concentration, as well as the size of alien mussels, significantly impact mussel filtration [12], inappropriate temperature and particle concentrations can greatly reduce filtration rates [43]. Thus, introducing time delays in biological models to accurately characterize the mussel filter-feeding rate is both reasonable and realistic [41, 45]. Moreover, as noted by May [23] and Ruan [30], these delays should reflect averages over past population densities. Building on model (1.1), this work further incorporates distributed delay to describe the time delay involved in converting available algae to viable mussel biomass

$$\begin{cases} \dfrac{\mathrm{d}A(t)}{\mathrm{d}t} = \big(A_{up} - A(t)\big)f - \dfrac{c}{h}A(t)M(t), \\ \dfrac{\mathrm{d}M(t)}{\mathrm{d}t} = e_1 cM(t)\displaystyle\int_{-\infty}^{t} G(t-s)A(s)\mathrm{d}s - \dfrac{dkM(t)}{k+M(t)} - EM(t). \end{cases} \tag{1.2}$$

In this model, the delay phenomenon is represented by the Gamma kernel function

$$G(s) = \frac{\alpha_1^m s^{m-1} e^{-\alpha_1 s}}{(m-1)!}, \quad m = 1,2,\ldots,$$

where m denotes the order of the delay kernel $G(t)$, and $\alpha_1>0$ indicates the rate of decay of the effect of past memories, which is associated with the mean time delay by

$$T_e=\int_0^{+\infty} tG(t)\mathrm{d}t=\frac{m}{\alpha_1}.$$

Specifically, two commonly used forms of the Gamma kernel function are the weak kernel $G(t)=\alpha_1 e^{-\alpha_1 t}$ (for $m=1$) and the strong kernel $G(t)=\alpha_1^2 te^{-\alpha_1 t}$ (for $m=2$).

Biofouling caused by mussels primarily results from adult mussels firmly adhering to underwater substrates using byssus secreted by their food glands, leading to extremely high population densities in invaded habitats [17]. According to Donnell *et al.* [28] and Kishore *et al.* [14], byssus production and performance in invasive mussels are influenced by various environmental factors, such as water temperature, pH, and metal ions, as well as environmental changes like seasonal fluctuations, water current velocities, and predator cues. Therefore, considering the environmental noise that relates environmental fluctuations to the colonization of invasive zebra mussels is essential. In contrast to the linear perturbation approach, recent research [20, 27, 45] have demonstrated that environmental fluctuations may depend on population sizes within ecosystems, known as nonlinear perturbations. When nonlinear perturbations are considered, Nguyen *et al.* [27] introduced a new method for treating a stochastic competition model with nonlinear diffusion components, primarily analyzing the behavior of solutions at the boundary. Yu *et al.* [45] proposed a stochastic chemostat model incorporating two distributed delays and nonlinear perturbations, studying the existence of a stationary distribution in their model and the extinction of plankton by constructing appropriate stochastic Lyapunov functions. Inspired by this previous work and considering the aggregation properties of mussels, we develop a stochastic version of model (1.2), expressed as follows:

$$\begin{cases} \mathrm{d}A(t)=\Big(\big(A_{up}-A(t)\big)f-\dfrac{c}{h}A(t)M(t)\Big)\mathrm{d}t+\sigma_{11}A\mathrm{d}B_1, & \text{(1.3a)}\\ \mathrm{d}M(t)=\Big(e_1cM(t)\displaystyle\int_{-\infty}^{t}G(t-s)A(s)\mathrm{d}s-\frac{dkM(t)}{k+M(t)}-EM(t)\Big)\mathrm{d}t+(\sigma_{21}+\sigma_{22}M)M\mathrm{d}B_2, & \text{(1.3b)}\end{cases}$$

where $B_1(t)$ and $B_2(t)$ are two independent standard Brownian motions defined on a complete probability space $(\Omega,\mathcal{F},\{\mathcal{F}_t\}_{t\geq 0},\mathbb{P})$ that satisfies the usual conditions [22]. Here, σ_{11}^2 represents the intensity of perturbation for algae, while σ_{21}^2 and σ_{22}^2 denote the intensities of linear and nonlinear perturbations for mussels, respectively.

The subsequent sections are organized as follows. In Section 2, using the linear chain technique, we transform model (1.3) into a $(m+3)$-dimensional model (2.1). Additionally, some necessary lemmas and preliminary results are presented in this section. Section 3 provides sufficient conditions for the persistence of mussel invasion in a stochastic environment, achieved by analyzing the existence of a stationary distribution in the stochastic model (1.3). In Section 4, we derive approximate expressions for the local density function of model (2.1) under the strong kernel function. Section 5 focuses on the sufficient

conditions for mussel invasion failure in model (2.1). Finally, the paper concludes with numerical simulations and discussions in Section 6.

2 Preliminaries

To facilitate our discussion, we will first introduce some notations and then transform the model into a more convenient form for analysis. We denote

$$I_n(t)=\int_{-\infty}^{t}\frac{(t-s)^{n-1}\alpha_1^n e^{-\alpha_1(t-s)}}{(n-1)!}A(s)\mathrm{d}s,\quad n=1,2,\ldots,m+1.$$

Then,

$$I_n(t)=\int_0^{+\infty}\frac{s^{n-1}e^{-s}}{(n-1)!}A\left(t-\frac{s}{\alpha_1}\right)\mathrm{d}s.$$

For the Eq. (1.3b), by applying the linear chain technique, we can transform it into the following form:

$$\begin{cases}\mathrm{d}A(t)=\Big(\big(A_{up}-A(t)\big)f-\dfrac{c}{h}A(t)M(t)\Big)\mathrm{d}t+\sigma_{11}A\mathrm{d}B_1,\\ \mathrm{d}M(t)=\left(e_1cI_{m+1}M(t)-\dfrac{dkM(t)}{k+M(t)}-EM(t)\right)\mathrm{d}t+(\sigma_{21}+\sigma_{22}M)M\mathrm{d}B_2,\\ \mathrm{d}I_1(t)=\alpha_1(A-I_1)\mathrm{d}t,\\ \mathrm{d}I_n(t)=\alpha_1(I_{n-1}-I_n)\mathrm{d}t,\quad n=2,3,\ldots,m+1.\end{cases}\tag{2.1}$$

We then derive a preliminary result concerning the existence and uniqueness of the global positive solution to Eq. (2.1), which is summarised in the following theorem.

Theorem 2.1. *For any initial value $X(0)=(A(0),M(0),I_1(0),\cdots,I_{m+1}(0))\in\mathbb{R}_+^{m+3}$, system* (2.1) *admits a unique solution $X(t)$ for $t\geq 0$, furthermore, this solution will remain in $\mathbb{R}_+^{m+3}$ with probability one.*

Proof. The coefficients of Eq. (2.1) satisfy the local Lipschitz condition. Therefore, for a given initial value $X(0)\in\mathbb{R}_+^{m+3}$, there exists a unique local solution $X(t)\in\mathbb{R}_+^{m+3}$ for $t\in[0,\tau_e)$, where τ_e represents the explosion time. To establish the global existence of the solution, we need to verify that $\tau_e=\infty$ almost surely (a.s.). To this end, let n_0 be sufficiently large such that every component of $X(0)$ lies within the interval $[1/n_0,n_0]$. For each integer $n\geq n_0$, the stopping time τ_n is defined as follows:

$$\tau_n=\inf\left\{0\leq t<\tau_e\,\middle|\,A(t)\notin\left(\frac{1}{n},n\right)\text{ or }M(t)\notin\left(\frac{1}{n},n\right)\text{ or }I_j(t)\notin\left(\frac{1}{n},n\right),\ j=1,2,\ldots,m+1\right\}.$$

Throughout this paper, we define $\inf\emptyset=\infty$, where $\emptyset$ is the empty set. Clearly, τ_n is a monotonically increasing function of the variable n. By letting $\tau_\infty=\lim_{n\to\infty}\tau_n$, we obtain

$\tau_\infty \le \tau_e$ a.s. Next, we prove that $\tau_\infty = \infty$ by contradiction. Assuming $\tau_\infty < +\infty$, then there exists constants $T>0, n_1 \ge n_0$ and $\varepsilon \in (0,1)$ such that

$$\mathbb{P}\{\tau_n \le T\} \ge \varepsilon, \quad \forall n \ge n_1.$$

First, consider the functions

$$V_{11} = \frac{1}{\theta+2}A^{\theta+2}(t) + \frac{1}{\theta}M^\theta(t) + \frac{1}{\alpha_1}\sum_{n=1}^{m+1}\frac{1}{2^{n-1}}I_n^2,$$
$$V_{12} = -\ln A(t) - \ln M(t) - \sum_{n=1}^{m+1}\ln I_n,$$

in which $0<\theta<1$ is a sufficiently small constant such that $f-(\theta+1)\sigma_{11}^2/2>0$. Obviously, defining $U_\rho = (\rho^{-1},\rho)^{m+3}$, we can get

$$\liminf_{\rho\to\infty, X\in\mathbb{R}_+^{m+3}\setminus U_\rho}\big(V_{11}(t)+V_{12}(t)\big) = \infty,$$

which implies that $V_{11}(t)+V_{12}(t)$ attains a lower bound at some point $\bar{X}\in\mathbb{R}_+^{m+3}$. Thus, a non-negative C^2-function $V_1 : \mathbb{R}_+^{m+3} \to \mathbb{R}_+$ a.s. can be constructed as follows:

$$V_1(t) = V_{11}(t) + V_{12}(t) - V_{11}(\bar{X}) - V_{12}(\bar{X}).$$

Direct calculations by Itô's formula and Young's inequality yields

$$\begin{aligned}\mathcal{L}\left(\frac{1}{\theta+2}A^{\theta+2}\right) &= A^{\theta+1}\left((A_{up}-A)f - \frac{c}{h}AM\right) + \frac{1}{2}(\theta+1)A^{\theta+2}\sigma_{11}^2 \\ &\le A_{up}fA^{\theta+1} - \left(f - \frac{1}{2}(\theta+1)\sigma_{11}^2\right)A^{\theta+2}, \end{aligned} \tag{2.2}$$

$$\mathcal{L}\left(\frac{1}{\theta}M^\theta\right) \le \frac{e_1 c\theta}{\theta+1}M^{\theta+1} + \frac{e_1 c}{\theta+1}I_{m+1}^{\theta+1} - \frac{1}{2}(1-\theta)\sigma_{22}^2 M^{\theta+2}, \tag{2.3}$$

$$\begin{aligned}\mathcal{L}\left(\frac{1}{\alpha_1}\sum_{n=1}^{m+1}\frac{1}{2^{n-1}}I_n^2\right) &= 2I_1(A-I_1) + \sum_{n=2}^{m+1}\frac{1}{2^{n-2}}\left(I_{n-1}I_n - I_n^2\right) \\ &\le A^2 - I_1^2 + \sum_{n=2}^{m+1}\frac{1}{2^{n-1}}\left(I_{n-1}^2 - I_n^2\right) \le A^2 - \sum_{n=1}^{m+1}\frac{1}{2^n}I_n^2. \end{aligned} \tag{2.4}$$

Combining (2.2)-(2.4), we have

$$\begin{aligned}\mathcal{L}V_{11} \le{}& A_{up}fA^{\theta+1} - \left(f - \frac{1}{2}(1+\theta)\sigma_{11}^2\right)A^{\theta+2} + \frac{e_1 c\theta}{\theta+1}M^{\theta+1} \\ &+ \frac{e_1 c}{\theta+1}I_{m+1}^{\theta+1} - \frac{1}{2}(1-\theta)\sigma_{22}^2 M^{\theta+2} + A^2 - \sum_{n=1}^{m+1}\frac{1}{2^n}I_n^2, \end{aligned} \tag{2.5}$$

$$\mathcal{L}V_{12} \le f + \frac{c}{h}M + \frac{1}{2}\sigma_{11}^2 + d + E + \frac{1}{2}\sigma_{21}^2 + \sigma_{21}\sigma_{22}M + \frac{1}{2}\sigma_{22}^2 M^2 + (m+1)\alpha_1. \tag{2.6}$$

Then it follows from (2.5) and (2.6) that

$$\mathcal{L}V_1 \leq f+\frac{1}{2}\sigma_{11}^2+d+E+(m+1)\alpha_1+\Delta_1,$$

where

$$\Delta_1 = \sup_{X\in\mathbb{R}_+^{m+3}}\left\{A_{up}fA^{\theta+1}-\left(f-\frac{1}{2}(\theta+1)\sigma_{11}^2\right)A^{\theta+2}+A^2+\frac{e_1c\theta}{\theta+1}M^{\theta+1}+\frac{c}{h}M \right.$$
$$\left. -\frac{1}{2}(1-\theta)\sigma_{22}^2M^{\theta+2}+\sigma_{21}\sigma_{22}M+\frac{1}{2}\sigma_{22}^2M^2+\frac{e_1c}{\theta+1}I_{m+1}^{\theta+1}-\sum_{n=1}^{m+1}\frac{1}{2^n}I_n^2\right\}.$$

Then, using the same idea as in [45] we complete the proof. □

3 Existence of a stationary distribution

In this section, we will examine the existence of an ergodic stationary distribution of system (2.1).

Theorem 3.1. *Given initial value $X(0)\in\mathbb{R}_+^{m+3}$, let $X(t)$ be the corresponding solution of system* (2.1). *Then $X(t)$ has a unique ergodic stationary distribution $\omega(\cdot)$ on $\mathbb{R}_+^{m+3}$ if $R_{01}>1$, where*

$$R_{01}=\frac{A_{up}}{(E+d+\sigma_{21}^2/2)/(e_1c)+A_{up}\sigma_{11}^2/2}.$$

Proof. We will use Theorem 2.1 and Lemma A.1 with $\mathbb{R}_+^\ell=\mathbb{R}_+^{m+3}$ to prove our conclusion for system (2.1). It is easy to verify that assumptions (A.2) and (A.3) are satisfied. The subsequent step is to construct an appropriate bounded set $E_\varepsilon\subseteq\mathbb{R}_+^{m+3}$ over which we have $\mathcal{L}V\leq -1$. Define a C^2-function $V_2(A,M,I_1,\cdots,I_{m+1}):\mathbb{R}_+^{m+3}\to\mathbb{R}$ by

$$V_2(t)=V_{11}+M_0V_{21}+V_{22},$$

where

$$V_{21}=A-A_{up}-A_{up}\ln\frac{A}{A_{up}}-\frac{1}{\alpha_1}\sum_{n=1}^{m+1}I_n-\frac{1}{e_1c}\ln M-\frac{1}{f}A,$$
$$V_{22}=-\ln A-\sum_{n=1}^{m+1}\ln I_n,$$

and V_{11} is given in Theorem 2.1. Clearly, there exists a sufficiently large constant $M_0>0$ such that

$$-M_0(R_{01}-1)\left(\frac{1}{e_1c}\left(E+d+\frac{1}{2}\sigma_{21}^2\right)+\frac{1}{2}A_{up}\sigma_{11}^2\right)+\Psi\leq -2,$$

where

$$\Psi=\sup_{X\in\mathbb{R}_+^{m+3}}\Big\{f+\frac{1}{2}\sigma_{11}^2+(m+1)\alpha_1+\frac{c}{h}M+\frac{e_1c\theta}{\theta+1}M^{\theta+1}+A^2-\frac{1}{4}(1-\theta)\sigma_{22}^2M^{\theta+2}$$
$$+A_{up}fA^{\theta+1}-\frac{1}{2}\left(f-\frac{1}{2}(\theta+1)\sigma_{11}^2\right)A^{\theta+2}+\frac{e_1c}{\theta+1}I_{m+1}^{\theta+1}-\sum_{n=1}^{m+1}\frac{1}{2^n}I_n^2\Big\}.$$

Applying the Itô's formula, there are

$$\begin{aligned}\mathcal{L}V_{11}\leq{}&A_{up}fA^{\theta+1}-\left(f-\frac{1}{2}(\theta+1)\sigma_{11}^2\right)A^{\theta+2}+\frac{e_1c\theta}{\theta+1}M^{\theta+1}\\&+\frac{e_1c}{\theta+1}I_{m+1}^{\theta+1}-\frac{1}{2}(1-\theta)\sigma_{22}^2M^{\theta+2}+A^2-\sum_{n=1}^{m+1}\frac{1}{2^n}I_n^2,\end{aligned}\tag{3.1}$$

$$\begin{aligned}\mathcal{L}V_{21}\leq{}&-\frac{(A_{up}-A)^2f}{A}+\frac{cA_{up}}{h}M+\frac{1}{2}A_{up}\sigma_{11}^2-A+\frac{dk}{e_1c(k+M)}\\&+\frac{E}{e_1c}+\frac{\sigma_{21}^2}{2e_1c}+\frac{\sigma_{21}\sigma_{22}}{e_1c}M+\frac{\sigma_{22}^2}{2e_1c}M^2+A-A_{up}+\frac{c}{fh}AM\\\leq{}&-\left(A_{up}-\frac{1}{2}A_{up}\sigma_{11}^2-\frac{E+d}{e_1c}-\frac{\sigma_{21}^2}{2e_1c}\right)+\frac{\sigma_{22}^2}{2e_1c}M^2\\&+\left(\frac{\sigma_{21}\sigma_{22}}{e_1c}+\frac{cA_{up}}{h}+\frac{c}{fh}A\right)M-\frac{(A_{up}-A)^2f}{A},\end{aligned}\tag{3.2}$$

$$\mathcal{L}V_{22}=-\frac{A_{up}f}{A}+f+\frac{c}{h}M+\frac{1}{2}\sigma_{11}^2-\frac{\alpha_1}{I_1}A+(m+1)\alpha_1-\alpha_1\sum_{n=2}^{m+1}\frac{I_{n-1}}{I_n}.\tag{3.3}$$

Noting that

$$\frac{cA_{up}}{h}+\frac{c}{fh}A+\frac{\sigma_{21}\sigma_{22}}{e_1c}\leq\frac{cA_{up}}{h}+\frac{cA_{up}}{fh}+\frac{\sigma_{21}\sigma_{22}}{e_1c}=:\Delta_2,\tag{3.4}$$

and combining (3.1)-(3.4), we can obtain

$$\begin{aligned}\mathcal{L}V_2\leq{}&M_0\left(-(R_{01}-1)\left(\frac{1}{e_1c}\left(E+d+\frac{1}{2}\sigma_{21}^2\right)+\frac{1}{2}A_{up}\sigma_{11}^2\right)+\Delta_2M+\frac{\sigma_{21}^2}{2e_1c}M^2\right)\\&-\frac{A_{up}f}{A}-\frac{1}{2}\left(f-\frac{1}{2}(\theta+1)\sigma_{11}^2\right)A^{\theta+2}-\frac{\alpha_1A}{I_1}-\frac{1}{4}(1-\theta)\sigma_{22}^2M^{\theta+2}\\&-\alpha_1\sum_{n=2}^{m+1}\frac{I_{n-1}}{I_n}-\sum_{n=1}^{m+1}\frac{1}{2^{n+1}}I_n^2+\Psi.\end{aligned}$$

Furthermore, we can construct an compact subset E_ε as follows:

$$E_\varepsilon=\left\{X(t)\in\mathbb{R}_+^{m+3}\,\middle|\,\varepsilon\leq A\leq\frac{1}{\varepsilon},\varepsilon\leq M\leq\frac{1}{\varepsilon},\varepsilon^{n+1}\leq I_n\leq\frac{1}{\varepsilon^{n+1}}\right\},$$

where $n=1,2,\ldots,m+1$ and $\varepsilon>0$ is a sufficiently small constant that satisfies the following inequalities:

$$\min\left\{\frac{A_{up}f}{\varepsilon},\frac{\alpha_1}{\varepsilon},\frac{\alpha_1}{\varepsilon^n},\frac{1}{2}\left(f-\frac{1}{2}(1+\theta)\sigma_{11}^2\right)\frac{1}{\varepsilon^{\theta+2}},\frac{1}{2^{n+1}\varepsilon^2}\right\}\geq\Psi_1+1, \tag{3.5}$$

$$M_0\left(-\frac{1}{e_1c}\left(E+d+\frac{1}{2}\sigma_{21}^2\right)+\frac{1}{2}A_{up}\sigma_{11}^2+\Delta_2\varepsilon+\frac{\sigma_{21}^2\varepsilon^2}{2e_1c}\right)+\Psi\leq-1, \tag{3.6}$$

$$\Psi_2-\frac{\sigma_{22}^2}{8\varepsilon^{\theta+2}}(1-\theta)\leq-1. \tag{3.7}$$

Here Ψ_1 and Ψ_2 are constants given in **Case 1** and **Case 6**, respectively. To facilitate our discussion, we divide the set $E_\varepsilon^c=\mathbb{R}_+^{m+3}\backslash E_\varepsilon$ into the following $2m+6$ subsets:

$$\begin{aligned}
&E_\varepsilon^1=\left\{X(t)\in\mathbb{R}_+^{m+3}:0<A(t)<\varepsilon\right\},\\
&E_\varepsilon^2=\left\{X(t)\in\mathbb{R}_+^{m+3}:0<M(t)<\varepsilon\right\},\\
&E_\varepsilon^3=\left\{X(t)\in\mathbb{R}_+^{m+3}:0<I_1(t)<\varepsilon^2\right\},\\
&E_\varepsilon^{n+2}=\left\{X(t)\in\mathbb{R}_+^{m+3}:0<I_n(t)<\varepsilon^{n+1},I_{n-1}(t)>\varepsilon^n,n=2,3,\ldots,m+1\right\},\\
&E_\varepsilon^{m+4}=\left\{X(t)\in\mathbb{R}_+^{m+3}:A(t)>\frac{1}{\varepsilon}\right\},\\
&E_\varepsilon^{m+5}=\left\{X(t)\in\mathbb{R}_+^{m+3}:M(t)>\frac{1}{\varepsilon}\right\},\\
&E_\varepsilon^{m+n+5}=\left\{X(t)\in\mathbb{R}_+^{m+3}:I_n(t)>\frac{1}{\varepsilon},n=1,2,\ldots,m+1\right\}.
\end{aligned}$$

And then, we will show $\mathcal{L}V_2\leq-1$ in each E_ε^j, $j=1,2,\ldots,2m+6$ implying the conclusion on E_ε^c. We have the following cases to consider:

Case 1. If $X(t)\in E_\varepsilon^1$, we have

$$\begin{aligned}
\mathcal{L}V_2&\leq M_0\left(\Delta_2M+\frac{\sigma_{21}^2}{2e_1c}M^2\right)-\frac{A_{up}f}{A}-\frac{1}{4}(1-\theta)\sigma_{22}^2M^{\theta+2}+\Psi\\
&\leq\Psi_1-\frac{A_{up}f}{A}\leq\Psi_1-\frac{A_{up}f}{\varepsilon}\leq-1,
\end{aligned}$$

where

$$\Psi_1=\sup_{X\in\mathbb{R}_+^{m+3}}\left\{-\frac{1}{4}(1-\theta)\sigma_{22}^2M^{\theta+2}+M_0\left(\Delta_2M+\frac{\sigma_{21}^2}{2e_1c}M^2\right)+\Psi\right\}.$$

Case 2. If $X(t)\in E_\varepsilon^2$, we have

$$\begin{aligned}
\mathcal{L}V_2&\leq M_0\left(-\frac{1}{e_1c}\left(E+d+\frac{1}{2}\sigma_{21}^2\right)+\frac{1}{2}A_{up}\sigma_{11}^2+\Delta_2M+\frac{\sigma_{21}^2}{2e_1c}M^2\right)+\Psi\\
&\leq M_0\left(-\frac{1}{e_1c}\left(E+d+\frac{1}{2}\sigma_{21}^2\right)+\frac{1}{2}A_{up}\sigma_{11}^2+\Delta_2\varepsilon+\frac{\sigma_{21}^2}{2e_1c}\varepsilon^2\right)+\Psi\leq-1.
\end{aligned}$$

Case 3. For any $X(t)\in E_\varepsilon^3$,

$$\mathcal{L}V_2\le\Psi_1-\alpha_1\frac{A}{I_1}\le\Psi_1-\frac{\alpha_1\varepsilon}{\varepsilon^2}\le-1.$$

Case 4. For any $X(t)\in E_\varepsilon^{n+2}$,

$$\mathcal{L}V_2\le\Psi_1-\alpha_1\frac{I_{n-1}}{I_n}\le\Psi_1-\alpha_1\frac{\varepsilon^n}{\varepsilon^{n+1}}\le-1.$$

Case 5. For any $X(t)\in E_\varepsilon^{m+4}$,

$$\begin{aligned}\mathcal{L}V_2&\le M_0\left[\Delta_2M+\frac{\sigma_{21}^2}{2e_1c}M^2\right]-\frac{1}{2}\left(f-\frac{1}{2}(\theta+1)\sigma_{11}^2\right)A^{\theta+2}-\frac{1}{4}(1-\theta)\sigma_{22}^2M^{\theta+2}+\Psi\\&\le\Psi_1-\frac{1}{2}\left(f-\frac{1}{2}(\theta+1)\sigma_{11}^2\right)A^{\theta+2}\\&\le\Psi_1-\frac{1}{2}\left(f-\frac{1}{2}(\theta+1)\sigma_{11}^2\right)\frac{1}{\varepsilon^{\theta+2}}\le-1.\end{aligned}$$

Case 6. If $X(t)\in E_\varepsilon^{m+5}$,

$$\begin{aligned}\mathcal{L}V_2&\le M_0\left[\Delta_2M+\frac{\sigma_{21}^2}{2e_1c}M^2\right]-\frac{1}{4}(1-\theta)\sigma_{22}^2M^{\theta+2}+\Psi\\&\le\Psi_2-\frac{1}{8}(1-\theta)\sigma_{22}^2M^{\theta+2}\\&\le\Psi_2-\frac{1}{8}(1-\theta)\sigma_{22}^2\frac{1}{\varepsilon^{\theta+2}}\le-1,\end{aligned}$$

where

$$\Psi_2=\sup_{X(t)\in\mathbb{R}_+^{m+3}}\left\{-\frac{1}{8}(1-\theta)\sigma_{22}^2M^{\theta+2}+M_0\left[\Delta_2M+\frac{\sigma_{21}^2}{2e_1c}M^2\right]+\Psi\right\}.$$

Case 7. If $X(t)\in E_\varepsilon^{m+n+5}$,

$$\begin{aligned}\mathcal{L}V_2&\le M_0\left(\Delta_2M+\frac{\sigma_{21}^2}{2e_1c}M^2\right)-\sum_{n=1}^{m+1}\frac{1}{2^{n+1}}I_n^2-\frac{1}{4}(1-\theta)\sigma_{22}^2M^{\theta+2}+\Psi\\&\le\sup_{X(t)\in\mathbb{R}_+^{m+3}}\left\{-\frac{1}{4}(1-\theta)\sigma_{22}^2M^{\theta+2}+M_0\left(\Delta_2M+\frac{\sigma_{21}^2}{2e_1c}M^2\right)+\Psi\right\}-\sum_{n=1}^{m+1}\frac{I_n^2}{2^{n+1}}\\&\le\Psi_1-\frac{1}{2^{n+1}}\frac{1}{\varepsilon^2}\le-1.\end{aligned}$$

Putting all the cases together, we obtain $\mathcal{L}V_2\le-1$ for any $(A,M,I_1,I_2,\cdots,I_{m+1})\in E_\varepsilon^c$, which means Lemma A.1 holds. Hence, the solution $(A,M,I_1,I_2,\cdots,I_{m+1})\in\mathbb{R}_+^{m+3}$ is ergodic and possesses a unique stationary distribution $\omega(\cdot)$. This completes the proof of theorem. □

4 Probability density function around a quasi-endemic equilibrium X^*

Given that the existence of a stationary solution may not fully capture the statistical properties of system (2.1), this section focuses on deriving the probability density function associated with the stationary solution of system (2.1). Before doing so, we first define

$$R_{02}=\frac{e_1cA_{up}f}{\left(f+\sigma_{11}^2/2\right)\left(d+E+\sigma_{21}^2/2\right)}, \tag{4.1}$$

and introduce two equivalent forms of system (2.1) by transformations.

4.1 Main equivalent transformations of system (2.1)

Let $v_1=\ln A, v_2=\ln M, v_{n+2}=\ln I_n$ for any $n=1,2,\ldots,m+1$. Applying the Itô's formula to v_n, we obtain

$$\begin{cases} \mathrm{d}v_1=\left(A_{up}fe^{-v_1}-f-\dfrac{1}{2}\sigma_{11}^2-\dfrac{c}{h}e^{v_2}\right)\mathrm{d}t+\sigma_{11}\mathrm{d}B_1,\\ \mathrm{d}v_2=\left(e_1ce^{v_{m+3}}-\dfrac{dk}{k+e^{v_2}}-E-\dfrac{1}{2}\left(\sigma_{21}+\sigma_{22}e^{v_2}\right)^2\right)\mathrm{d}t+\left(\sigma_{21}+\sigma_{22}e^{v_2}\right)\mathrm{d}B_2,\\ \mathrm{d}v_3=\left(\alpha_1e^{v_1-v_3}-\alpha_1\right)\mathrm{d}t,\\ \mathrm{d}v_n=\left(\alpha_1e^{v_{n-1}-v_n}-\alpha_1\right)dt,\quad n=4,5,\ldots,m+3. \end{cases} \tag{4.2}$$

By solving

$$\begin{cases} A_{up}fe^{-v_1^*}-\left(f+\dfrac{1}{2}\sigma_{11}^2\right)-\dfrac{c}{h}e^{v_2^*}=0,\\ e_1ce^{v_{m+3}^*}-\dfrac{dk}{k+e^{v_2^*}}-E-\dfrac{1}{2}\left(\sigma_{21}+\sigma_{22}e^{v_2^*}\right)^2=0,\\ \alpha_1e^{v_1^*-v_3^*}-\alpha_1=0,\\ \alpha_1e^{v_{n-1}^*-v_n^*}-\alpha_1=0,\quad n=4,\ldots,m+3, \end{cases} \tag{4.3}$$

we obtain a quasi-equilibrium as

$$X^*=\left(A^*,M^*,I_1^*,\cdots,I_{m+1}^*\right)^\top=\left(e^{v_1^*},e^{v_2^*},\cdots,e^{v_{m+3}^*}\right)^\top.$$

A direct calculation shows that

$$A^*=I_1^*=I_2^*=\cdots=I_{m+1}^*=\frac{A_{up}f}{f+\sigma_{11}^2/2+cM^*/h},$$

and M^* is the solution of

$$-\tilde{a}_1M^4-\tilde{a}_2M^3-\tilde{a}_3M^2-\tilde{a}_4M+\tilde{a}_5=0, \tag{4.4}$$

where

$$\tilde{a}_1=\frac{c\sigma_{22}^2}{2h},\quad \tilde{a}_2=\frac{\sigma_{21}\sigma_{22}c}{h}+\frac{1}{2}\sigma_{22}^2\left(\frac{kc}{h}+f+\frac{1}{2}\sigma_{11}^2\right),$$
$$\tilde{a}_3=\frac{Ec}{h}+\frac{1}{2}\sigma_{22}^2\left(f+\frac{1}{2}\sigma_{11}^2\right)k+\frac{c\sigma_{21}^2}{2h}+\sigma_{21}\sigma_{22}\left(\frac{kc}{h}+f+\frac{1}{2}\sigma_{11}^2\right),$$
$$\tilde{a}_4=-e_1cA_{up}f+\frac{kc}{h}(d+E)+E\left(f+\frac{1}{2}\sigma_{11}^2\right)+\frac{1}{2}\sigma_{21}^2\left(\frac{kc}{h}+f+\frac{1}{2}\sigma_{11}^2\right)+\sigma_{21}\sigma_{22}\left(f+\frac{1}{2}\sigma_{11}^2\right)k,$$
$$\tilde{a}_5=e_1cA_{up}fk-k\left(f+\frac{1}{2}\sigma_{11}^2\right)\left(d+E+\frac{1}{2}\sigma_{21}^2\right).$$

Then, using the Descartes' rule of sign, we known that no matter whether the value of $\tilde{a}_4$ is positive or negative, Eq. (4.4) has a unique positive root, implying that (4.3) has a unique solution when $R_0^p>1$, that is, model (4.2) has a unique quasi-equilibrium if $R_0^p>1$.

Next, we study the property of (4.2) near the quasi-equilibrium X^*. To this end, we denote

$$B(t)=\big(B_1(t),B_2(t),0,\cdots,0\big)^\top,$$
$$U(t)=\big(u_1(t),u_2(t),\cdots,u_{m+3}(t)\big)^\top,$$

where $u_i=v_i-v_i^*, i=1,2,\ldots,m+3$. Then, we linearise (4.2) at X^* and obtain

$$\mathrm{d}U(t)=JU(t)\mathrm{d}t+\Lambda\mathrm{d}B(t), \tag{4.5}$$

where

$$J=\begin{pmatrix}-a_{11}&-a_{12}&0&0&\cdots&0&0\\0&-a_{22}&0&0&\cdots&0&a_{2,m+3}\\\alpha_1&0&-\alpha_1&0&\cdots&0&0\\0&0&\alpha_1&-\alpha_1&\cdots&0&0\\\vdots&\vdots&\vdots&\vdots&\ddots&\vdots&\vdots\\0&0&0&0&\cdots&\alpha_1&-\alpha_1\end{pmatrix},\quad \Lambda=\begin{pmatrix}\delta_1&0&0&0&\cdots&0&0\\0&\delta_2&0&0&\cdots&0&0\\0&0&0&0&\cdots&0&0\\0&0&0&0&\cdots&0&0\\\vdots&\vdots&\vdots&\vdots&\ddots&\vdots&\vdots\\0&0&0&0&\cdots&0&0\end{pmatrix},$$

and

$$a_{11}=A_{up}fe^{-v_1^*},\qquad a_{12}=\frac{c}{h}e^{v_2^*},$$
$$a_{22}=\sigma_{21}\sigma_{22}e^{v_2^*}+\frac{1}{2}\sigma_{22}^2e^{2v_2^*}-\frac{dke^{v_2^*}}{(k+e^{v_2^*})^2},\quad a_{2,m+3}=e_1ce^{v_{m+3}^*},$$
$$\delta_1=\sigma_{11},\qquad \delta_2=\sigma_{21}+\sigma_{22}e^{v_2^*}.$$

By the theory of Gardiner [7], the transient density function $\Phi(X(t),t)$ of the solution of system (4.5) governed by the following Fokker-Planck equation:

$$\frac{\partial\Phi}{\partial t}=-\sum_{i=1}^{m+3}\frac{\partial}{\partial u_i}\big[J^{(i)}U(t)\Phi\big(U(t),t\big)\big]+\sum_{i=1}^{2}\frac{\delta_i^2}{2}\frac{\partial^2\Phi}{\partial u_i^2} \tag{4.6}$$

for any time t, where $J^{(i)}$ represents the i-th row vector of J. By the standard argument of Roozen [29], system (4.5) with initial value $U(0)$ has a unique explicit solution

$$U(t)=e^{Jt}U(0)+\int_0^t e^{J(t-s)}\Lambda \mathrm{d}B(s).$$

Note that Λ is a constant matrix, therefore $\int_0^t e^{J(t-s)}\Lambda \mathrm{d}B(s)$ follows a Gaussian distribution. This implies that system (4.5) has a unique invariant Gaussian distribution $F(\cdot)$, and the distribution of the solution $U(t)$ will converge to $F(\cdot)$ as $t\to\infty$. For simplicity, let

$$\Phi^*\big(U(t)\big)=C_u e^{-\frac{1}{2}U^\top QU}$$

represent the density function of $F(\cdot)$, where C_u is a positive constant satisfying the normalization condition

$$\int_{\mathbb{R}_+^{m+3}}\Phi^*(U)\mathrm{d}u_1\cdots\mathrm{d}u_{m+3}=1$$

and Q is a real symmetric matrix. In this case, the transient density function $\Phi(U(t),t)$ converges to the invariant density function $\Phi^*(X(t))$, i.e.

$$\int_{\mathbb{R}^{m+3}}\big|\Phi\big(U(t),t\big)-\Phi^*\big(U(t)\big)\big|\mathrm{d}U=0.$$

Combining $\partial\Phi^*/\partial t=0$ and Eq. (4.6), the invariant density function $\Phi^*(U(t))$ satisfies the following equation:

$$\begin{aligned}&\frac{\partial}{\partial u_1}[(-a_{11}u_1-a_{12}u_2)\Phi^*]+\frac{\partial}{\partial u_2}[(-a_{22}u_2+a_{2,m+3}u_{m+3})\Phi^*]\\&\quad+\frac{\partial}{\partial u_3}[(\alpha_1u_1-\alpha_1u_3)\Phi^*]+\sum_{i=4}^{m+3}\frac{\partial}{\partial u_i}[(\alpha_1u_{i-1}-\alpha_1u_i)\Phi^*]-\frac{\delta_1^2}{2}\frac{\partial^2\Phi^*}{\partial u_1^2}-\frac{\delta_2^2}{2}\frac{\partial^2\Phi^*}{\partial u_2^2}=0.\end{aligned}\tag{4.7}$$

Substituting the expression of Φ^* into (4.7), Q satisfies the following algebraic equation:

$$Q\Lambda^2Q+J^\top Q+QJ=0.$$

If Q is a inverse matrix, by letting $\Sigma=Q^{-1}$, we derive

$$\Lambda^2+J\Sigma+\Sigma J^\top=0.\tag{4.8}$$

Consider two algebraic equations as follows:

$$\Lambda_i^2+J\Sigma_i+\Sigma_iJ^\top=0,\quad i=1,2,$$

where $\Lambda_1=\mathrm{diag}(\delta_1,0,0,\cdots,0)$ and $\Lambda_2=\mathrm{diag}(0,\delta_2,0,\cdots,0)$. Note that $\Lambda^2=\Lambda_1^2+\Lambda_2^2$, we can then apply the finite independent superposition principle [36] to derive $\Sigma=\Sigma_1+\Sigma_2$.

According to [30, 40], time delay phenomena, in reality, can be effectively simulated using two common distributed kernel functions: the weak kernel and the strong kernel. For the weak kernel case, the relevant calculation methods can be referred to [8]. In this study, we focus exclusively on the probability density function of system (2.1) when utilizing the strong kernel.

4.2 Density function of the strong kernel case

In the case of the strong kernel, a four-order real symmetric matrix of the diffusion matrix J is described by

$$J^{(4)}=\begin{pmatrix}-a_{11} & -a_{12} & 0 & 0\\ 0 & -a_{22} & 0 & a_{24}\\ \alpha_1 & 0 & -\alpha_1 & 0\\ 0 & 0 & \alpha_1 & -\alpha_1\end{pmatrix},$$

where a_{11},a_{12},a_{22} and a_{24} are the same as those in (4.5). The corresponding characteristic polynomial of $J^{(4)}$ is described by

$$\psi_J=\lambda^4+q_1\lambda^3+q_2\lambda^2+q_3\lambda+q_4, \tag{4.9}$$

where

$$\begin{aligned} &q_1=2\alpha_1+a_{11}+a_{22}, && q_2=\alpha_1^2+2\alpha_1(a_{11}+a_{22})+a_{11}a_{22},\\ &q_3=\alpha_1^2(a_{11}+a_{22})+2\alpha_1a_{11}a_{22}, && q_4=(a_{11}a_{22}+a_{12}a_{24})\alpha_1^2.\end{aligned}$$

We first make the following necessary assumptions.

Assumption 4.1. $R_{02}>1, a_{22}>0$ and $2a_{11}a_{22}>a_{12}a_{24}$.

Theorem 4.1. *Under Assumption* 4.1*, for any initial value* $(A(0),M(0),I_1(0),I_2(0))\in\mathbb{R}^4_+$*, the solution* $(A(t),M(t),I_1(t),I_2(t))$ *of system* (2.1) *with strong kernel will have a log-normal probability density function* $\Phi^*(A,M,I_1,I_2)$ *around* X^**, which takes the form of*

$$\Phi^*(A,M,I_1,I_2)=\frac{1}{4\pi^2\sqrt{|\Sigma|}AMI_1I_2}e^{-\frac{1}{2}G\Sigma^{-1}G^\top}, \tag{4.10}$$

where

$$G=\left(\ln\frac{A}{A^*},\ln\frac{M}{M^*},\ln\frac{I_1}{I_1^*},\ln\frac{I_2}{I_2^*}\right),$$

and Σ *is a positive definite matrix and satisfies*

$$\Sigma=\Sigma_1+\Sigma_2=\frac{a_{24}^2\alpha_1^4\delta_1^2}{2}(P_1B_1)^{-1}\Pi\big((P_1B_1)^{-1}\big)^\top+\frac{a_{12}^2\alpha_1^4\delta_2^2}{2}(P_2B_2)^{-1}\Pi\big((P_2B_2)^{-1}\big)^\top.$$

Here

$$P_1=\begin{pmatrix}a_{24}\alpha_1^2 & -a_{24}\alpha_1(a_{22}+2\alpha_1) & a_{24}\big(a_{22}^2+a_{22}\alpha_1+\alpha_1^2\big) & -a_{22}^3\\ 0 & a_{24}\alpha_1 & -a_{24}(a_{22}+\alpha_1) & a_{22}^2\\ 0 & 0 & a_{24} & -a_{22}\\ 0 & 0 & 0 & 1\end{pmatrix},\quad B_1=\begin{pmatrix}1&0&0&0\\0&0&1&0\\0&0&0&1\\0&1&0&0\end{pmatrix},$$

$$P_2=\begin{pmatrix}-a_{12}\alpha_1^2 & -\alpha_1^2(a_{11}+2\alpha_1) & 3\alpha_1^3 & -\alpha_1^3\\ 0 & \alpha_1^2 & -2\alpha_1^2 & \alpha_1^2\\ 0 & 0 & \alpha_1 & -\alpha_1\\ 0 & 0 & 0 & 1\end{pmatrix},\qquad B_2=\begin{pmatrix}0&1&0&0\\1&0&0&0\\0&0&1&0\\0&0&0&1\end{pmatrix},$$

$$\Pi=\begin{pmatrix} \frac{q_1q_4-q_2q_3}{q_1^2q_4-q_1q_2q_3+q_3^2} & 0 & \frac{q_3}{q_1^2q_4-q_1q_2q_3+q_3^2} & 0 \\ 0 & -\frac{q_3}{q_1^2q_4-q_1q_2q_3+q_3^2} & 0 & \frac{q_1}{q_1^2q_4-q_1q_2q_3+q_3^2} \\ \frac{q_3}{q_1^2q_4-q_1q_2q_3+q_3^2} & 0 & -\frac{q_1}{q_1^2q_4-q_1q_2q_3+q_3^2} & 0 \\ 0 & \frac{q_1}{q_1^2q_4-q_1q_2q_3+q_3^2} & 0 & -\frac{q_1q_2-q_3}{(q_1^2q_4-q_1q_2q_3+q_3^2)q_4} \end{pmatrix},$$

where $q_i, i=1,2,3,4$ *is given in* (4.9).

4.3 Proof of Theorem 4.1

Proof. Under Assumption 4.1, we can obtain $q_i>0, q_1q_2-q_3>0$ and $q_3(q_1q_2-q_3)-q_1^2q_4>0$. By applying the Routh-Hurwitz criterion, it can be concluded that $J^{(4)}$ has eigenvalues with all negative real parts. Furthermore, we can obtain the explicit form of Σ in two steps.

Step 1. For the algebraic equation

$$\Lambda_1^2+J^{(4)}\Sigma_1+\Sigma_1J^{(4)\top}=0, \tag{4.11}$$

letting

$$J_1=B_1J^{(4)}B_1^{-1}=\begin{pmatrix} -a_{11} & 0 & 0 & -a_{12} \\ \alpha_1 & -\alpha_1 & 0 & 0 \\ 0 & \alpha_1 & -\alpha_1 & 0 \\ 0 & 0 & a_{24} & -a_{22} \end{pmatrix},$$

where the first elimination matrix

$$B_1=\begin{pmatrix} 1 & 0 & 0 & 0 \\ 0 & 0 & 1 & 0 \\ 0 & 0 & 0 & 1 \\ 0 & 1 & 0 & 0 \end{pmatrix}.$$

According to Appendix B, we construct a standardized transformation matrix

$$P_1=\begin{pmatrix} a_{24}\alpha_1^2 & -a_{24}\alpha_1(a_{22}+2\alpha_1) & a_{24}\left(a_{22}^2+a_{22}\alpha_1+\alpha_1^2\right) & -a_{22}^3 \\ 0 & a_{24}\alpha_1 & -a_{24}(a_{22}+\alpha_1) & a_{22}^2 \\ 0 & 0 & a_{24} & -a_{22} \\ 0 & 0 & 0 & 1 \end{pmatrix},$$

and let $M_1=P_1J_1P_1^{-1}$. Then, we obtain a standard R_4 matrix

$$M_1=\begin{pmatrix} -q_1 & -q_2 & -q_3 & -q_4 \\ 1 & 0 & 0 & 0 \\ 0 & 1 & 0 & 0 \\ 0 & 0 & 1 & 0 \end{pmatrix}.$$

Furthermore, (4.11) can be equivalently transformed into

$$(P_1B_1)\Lambda_1^2(P_1B_1)^\top + M_1(P_1B_1)\Sigma_1(P_1B_1)^\top + (P_1B_1)\Sigma_1(P_1B_1)^\top M_1^\top = 0.$$

By virtue of a similar transformation of the matrix, M_1 also possesses eigenvalues with all negative real parts. Hence, as shown in Lemma A.2, we can obtain that

$$(P_1B_1)\Sigma_1(P_1B_1)^\top = \frac{a_{24}^2\alpha_1^4\delta_1^2}{2}\Pi,$$

where

$$\Pi = \begin{pmatrix} \frac{q_1q_4-q_2q_3}{q_1^2q_4-q_1q_2q_3+q_3^2} & 0 & \frac{q_3}{q_1^2q_4-q_1q_2q_3+q_3^2} & 0 \\ 0 & -\frac{q_3}{q_1^2q_4-q_1q_2q_3+q_3^2} & 0 & \frac{q_1}{q_1^2q_4-q_1q_2q_3+q_3^2} \\ \frac{q_3}{q_1^2q_4-q_1q_2q_3+q_3^2} & 0 & -\frac{q_1}{q_1^2q_4-q_1q_2q_3+q_3^2} & 0 \\ 0 & \frac{q_1}{q_1^2q_4-q_1q_2q_3+q_3^2} & 0 & -\frac{q_1q_2-q_3}{(q_1^2q_4-q_1q_2q_3+q_3^2)q_4} \end{pmatrix}.$$

Thus,

$$\Sigma_1 = \frac{a_{24}^2\alpha_1^4\delta_1^2}{2}(P_1B_1)^{-1}\Pi\big((P_1B_1)^{-1}\big)^\top$$

remains a positive definite matrix.

Step 2. We are now positioned to examine the following algebraic equation:

$$\Lambda_2^2 + J^{(4)}\Sigma_2 + \Sigma_2 J^{(4)\top} = 0. \tag{4.12}$$

Similarly, define $J_2 = B_2J^{(4)}B_2^{-1}$, we can calculate that

$$J_2 = \begin{pmatrix} -a_{22} & 0 & 0 & a_{24} \\ -a_{12} & -a_{11} & 0 & 0 \\ 0 & \alpha_1 & -\alpha_1 & 0 \\ 0 & 0 & \alpha_1 & -\alpha_1 \end{pmatrix},$$

where

$$B_2 = \begin{pmatrix} 0 & 1 & 0 & 0 \\ 1 & 0 & 0 & 0 \\ 0 & 0 & 1 & 0 \\ 0 & 0 & 0 & 1 \end{pmatrix}.$$

As in Step 1, we can obtain a standard transform matrix P_2 as the following:

$$P_2 = \begin{pmatrix} -a_{12}\alpha_1^2 & -\alpha_1^2(a_{11}+2\alpha_1) & 3\alpha_1^3 & -\alpha_1^3 \\ 0 & \alpha_1^2 & -2\alpha_1^2 & \alpha_1^2 \\ 0 & 0 & \alpha_1 & -\alpha_1 \\ 0 & 0 & 0 & 1 \end{pmatrix}.$$

Let $M_2 = P_2 J_2 P_2^{-1}$, we can obtain $M_2 = M_1$ is also a standard R_4 matrix. Thus, (4.12) can be transformed into the following equation:

$$(P_2B_2)\Lambda_2^2(P_2B_2)^\top + M_2(P_2B_2)\Sigma_2(P_2B_2)^\top + (P_2B_2)\Sigma_2(P_2B_2)^\top M_2^\top = 0.$$

Use Lemma A.2 again, we can obtain that

$$(P_2B_2)\Sigma_2(P_2B_2)^\top = \frac{a_{12}^2\alpha_1^4\delta_2^2}{2}\Pi.$$

Therefore,

$$\Sigma_2 = \frac{a_{12}^2\alpha_1^4\delta_2^2}{2}(P_2B_2)^{-1}\Pi\big((P_2B_2)^{-1}\big)^\top$$

is a positive definite matrix. Summarizing the previous steps, the probability density function $\Phi^*(A,M,I_1,I_2)$ of system (2.1) with strong kernel function around X^* is

$$\Phi^*(A,M,I_1,I_2) = \frac{1}{4\pi^2\sqrt{|\Sigma|}AMI_1I_2}e^{-\frac{1}{2}G\Sigma^{-1}G^\top},$$

where

$$G = -\frac{1}{2}\left(\ln\frac{A}{A^*}, \ln\frac{M}{M^*}, \ln\frac{I_1}{I_1^*}, \ln\frac{I_2}{I_2^*}\right),$$

and Σ is a positive definite covariance matrix and satisfies

$$\Sigma = \Sigma_1 + \Sigma_2 = \frac{a_{24}^2\alpha_1^4\delta_1^2}{2}(P_1B_1)^{-1}\Pi\big[(P_1B_1)^{-1}\big]^\top + \frac{a_{12}^2\alpha_1^4\delta_2^2}{2}(P_2B_2)^{-1}\Pi\big[(P_2B_2)^{-1}\big]^\top.$$

This completes the proof of theorem. □

5 Extinction

In this section, we will establish some theoretical results about the extinction of system (2.1). Denote

$$R_{03} = \frac{e_1cA_{up}}{E+\sigma_{21}^2/2} < 1.$$

We then have the following theorem.

Theorem 5.1. *Suppose that $R_{03}<1$. Then the solution $(A(t),M(t),I_1(t),\cdots,I_{m+1}(t))$ of system (2.1) with initial value $(A(0),M(0),I_1(0)\cdots,I_{m+1}(0)) \in \mathbb{R}_+^{m+3}$ has the following property:*

$$\limsup_{t\to\infty}\frac{\ln M(t)}{t} \le 0 \quad a.s.,$$

which shows the mussel species will exponentially extinct with probability one.

Proof. Considering the stochastic differential equation

$$\mathrm{d}\hat{A}(t)=\big((A_{up}-\hat{A})f\big)\mathrm{d}t+\sigma_{11}\hat{A}\mathrm{d}B_1$$

with the initial value $\hat{A}(0)=A(0)>0$. Based on the stochastic comparison theorem [11], we have $\hat{A}(t)\geq A(t)$ for any $t\geq 0$ a.s. By solving the Fokker-Planck equation and combining it with the strong law of large numbers [33], the process $\hat{A}(t)$ has ergodic property and we deduce that

$$\lim_{t\to+\infty}\frac{1}{t}\int_0^t\hat{A}(x)\mathrm{d}x=\int_0^t xh(x)\mathrm{d}x=A_{up}\quad\text{a.s.},\tag{5.1}$$

where

$$h(x)=\frac{b^a}{\Gamma(a)}x^{-(a+1)}e^{-\frac{b}{x}}$$

with

$$c_1=f+\frac{1}{2}\sigma_{11}^2,\quad a=\frac{2c_1}{\sigma_{11}^2},\quad b=\frac{2A_{up}f}{\sigma_{11}^2}.$$

Letting

$$V_3=\ln M(t)+\sum_{n=1}^{m+1}I_n=:V_{31}+V_{32},$$

and applying the Itô's formula to $\ln M(t)$, we have

$$\mathrm{d}V_{31}=\left(e_1cI_{m+1}-\frac{dk}{k+M}-E-\frac{1}{2}(\sigma_{21}+\sigma_{22}M)^2\right)\mathrm{d}t+(\sigma_{21}+\sigma_{22}M)\mathrm{d}B_2.$$

Through further calculations, we can obtain

$$\frac{1}{t}\ln\frac{M(t)}{M(0)}\leq\frac{e_1c}{t}\int_0^t I_{m+1}(s)\mathrm{d}s-E-\frac{1}{2t}\int_0^t(\sigma_{21}+\sigma_{22}M)^2\mathrm{d}s+\frac{1}{t}\int_0^t(\sigma_{21}+\sigma_{22}M)\mathrm{d}B_2.\tag{5.2}$$

Using the exponential martingale inequality, we get

$$\mathbb{P}\left\{\sup_{0\leq t\leq n}\left(\int_0^t(\sigma_{21}+\sigma_{22}M)\mathrm{d}B_2(s)-\frac{\varepsilon}{2}\int_0^t(\sigma_{21}+\sigma_{22}M)^2\mathrm{d}s\right)>\frac{2\ln n}{\varepsilon}\right\}\leq\frac{1}{n^2},\quad n\in\mathbb{Z}_+$$

for all $\varepsilon>0$. According to the Borel-Cantelli lemma, there exists an integer $n_0(\tau)>0$ such that for almost every $\tau\in\Omega$ and for all $n\geq n_0(\tau)$ and $t\in[n-1,n)$ a.s., we can get

$$\int_0^t(\sigma_{21}+\sigma_{22}M)\mathrm{d}B_2\leq\frac{2\ln n}{\varepsilon}+\frac{\varepsilon}{2}\int_0^t(\sigma_{21}+\sigma_{22}M)^2\mathrm{d}s.$$

This implies

$$\begin{aligned}&\frac{1}{t}\int_0^t(\sigma_{21}+\sigma_{22}M)\mathrm{d}B_2-\frac{1}{2t}\int_0^t(\sigma_{21}+\sigma_{22}M)^2\mathrm{d}s\\ \leq&\frac{2\ln n}{\varepsilon t}-\frac{1-\varepsilon}{2t}\int_0^t(\sigma_{21}+\sigma_{22}M)^2\mathrm{d}s\\ \leq&\frac{2\ln(t+1)}{\varepsilon t}-\frac{(1-\varepsilon)\sigma_{21}^2}{2}.\end{aligned}\tag{5.3}$$

On the other hand, considering $\mathrm{d}V_{32}=\alpha_1(A-I_{m+1})\mathrm{d}t$, we can further deduce that

$$\frac{\alpha_1}{t}\int_0^t I_{m+1}(s)\mathrm{d}s=\frac{\alpha_1}{t}\int_0^t A(s)\mathrm{d}s-\frac{1}{t}\left(\sum_{n=1}^{m+1}I_n(t)-\sum_{n=1}^{m+1}I_n(0)\right).\tag{5.4}$$

So combining (5.3) and (5.4) we can get

$$\begin{aligned}\frac{1}{t}\ln\frac{M(t)}{M(0)}\leq&\frac{e_1c}{t}\int_0^t A(s)\mathrm{d}s-\frac{e_1c}{\alpha_1 t}\left(\sum_{n=1}^{m+1}I_n(t)-\sum_{n=1}^{m+1}I_n(0)\right)\\ &-\frac{1}{t}\int_0^t\frac{dk}{k+M}\mathrm{d}s-E+\frac{2\ln(t+1)}{\varepsilon t}-\frac{(1-\varepsilon)\sigma_{21}^2}{2}.\end{aligned}\tag{5.5}$$

Letting $t\to\infty$ and taking the superior limit on both sides of (5.5), we can get

$$\limsup_{t\to\infty}\frac{1}{t}\ln M(t)\leq e_1cA_{up}-E-\frac{1}{2}\sigma_{21}^2+\frac{\varepsilon\sigma_{21}^2}{2}\quad\text{a.s.}$$

Thus, the assertion can be obtained by letting $\varepsilon\to0$. This completes the proof. □

6 Numerical simulations and discussions

In this section, we will illustrate our theoretical results via numerical simulations, using the high-order numerical method of Milstein [10]. The corresponding discretization equations of system (2.1) are

$$\begin{cases}A^{i+1}=A^i+\left((A_{up}-A^i)f-\dfrac{c}{h}A^iM^i\right)\Delta t+\dfrac{1}{2}\sigma_{11}^2A^i(\xi_{1,j}^2-1)\Delta t+\sigma_{11}A^i\sqrt{\Delta t}\xi_{1,j},\\ M^{i+1}=M^i+\left(e_1cI_{m+1}^iM^i-\dfrac{dkM^i}{k+M^i}-EM^i\right)\Delta t+(\sigma_{21}+\sigma_{22}M^i)M^i\sqrt{\Delta t}\xi_{2,j}\\ \qquad+\dfrac{1}{2}M^i(\sigma_{21}^2+3\sigma_{21}\sigma_{22}M^i+2\sigma_{22}^2(M^i)^2)(\xi_{2,j}^2-1)\Delta t,\\ I_1^{i+1}=I_1^i+\alpha_1(A^i-I_1^i)\Delta t,\\ I_n^{i+1}=I_n^i+\alpha_1(I_{n-1}^i-I_n^i)\Delta t,\quad n=2,3,\ldots,m+1,\end{cases}\tag{6.1}$$

where $\Delta t > 0$ is step size in time and $\xi_{i,j}$ $(i = 1,2)$ denotes the independent Gaussian random variable that follows the normal distribution $N(0,1)$ for $j = 1,2,\ldots,n$. (A^i, M^i) is the value of the ith iteration of the discretized equation. We select the parameters of system (2.1) as follows:

$$\begin{aligned} &A_{up}=400, \quad f=5, \quad c=0.1, \quad h=5, \qquad e_1=0.2,\\ &k=10, \qquad E=4, \quad d=2, \qquad \alpha_1=250. \end{aligned} \tag{6.2}$$

6.1 Species coexistence of model (2.1)

We primarily investigate the dynamical behavior of the species in model (2.1) from two perspectives: (i) an analysis of the stationary distribution of model (2.1) with the strong kernel, accompanied by simulations of the probability density function; and (ii) a discussion on the extinction of invasive mussels in model (2.1) with the strong kernel. Let the stochastic noises be defined as follows:

$$\sigma_{11}=0.1, \quad \sigma_{21}=1, \quad \sigma_{22}=0.001.$$

All other parameters and initial values remain consistent with those specified in (6.2). Under this setting of parameters and initial values, we obtain that

$$\begin{aligned} &R_{01}=\frac{2e_1cA_{up}}{e_1cA_{up}\sigma_{11}^2+2\left(E+d+\sigma_{21}^2/2\right)}=1.2232>1,\\ &f-\frac{1}{2}(\theta+1)\sigma_{11}^2>0. \end{aligned}$$

According to Theorem 3.1, system (2.1) admits a unique stationary distribution. The corresponding solutions of system (2.1) with the strong kernel, along with the frequency histograms, are presented in the left and right columns of Fig. 1, respectively. Additionally, we compute that

$$a_{22}=0.088>0, \quad q_1q_2-q_3>0, \quad q_3(q_1q_2-q_3)-q_1^2q_4>0, \quad R_{02}=1.2295>1,$$

and $X^*=(239.70,166.95,239.70,239.70)$. By Theorem 4.1, the distribution around X^* is approximately described by a four-dimensional log-normal probability density function $\Phi^*(A,M,I_1,I_2)$. The covariance matrix Σ is given by

$$\Sigma=\begin{pmatrix} 0.1946 & -0.2823 & 0.1919 & 0.1892\\ -0.2823 & 0.9845 & -0.2785 & -0.2747\\ 0.1919 & -0.2785 & 0.1919 & 0.1906\\ 0.1892 & -0.2748 & 0.1906 & 0.1906 \end{pmatrix}.$$

Then we have

$$\Phi^*(A,M,I_1,I_2)=\frac{57.2208}{AMI_1I_2}e^{-\frac{1}{2}G\Sigma^{-1}G^\top},$$

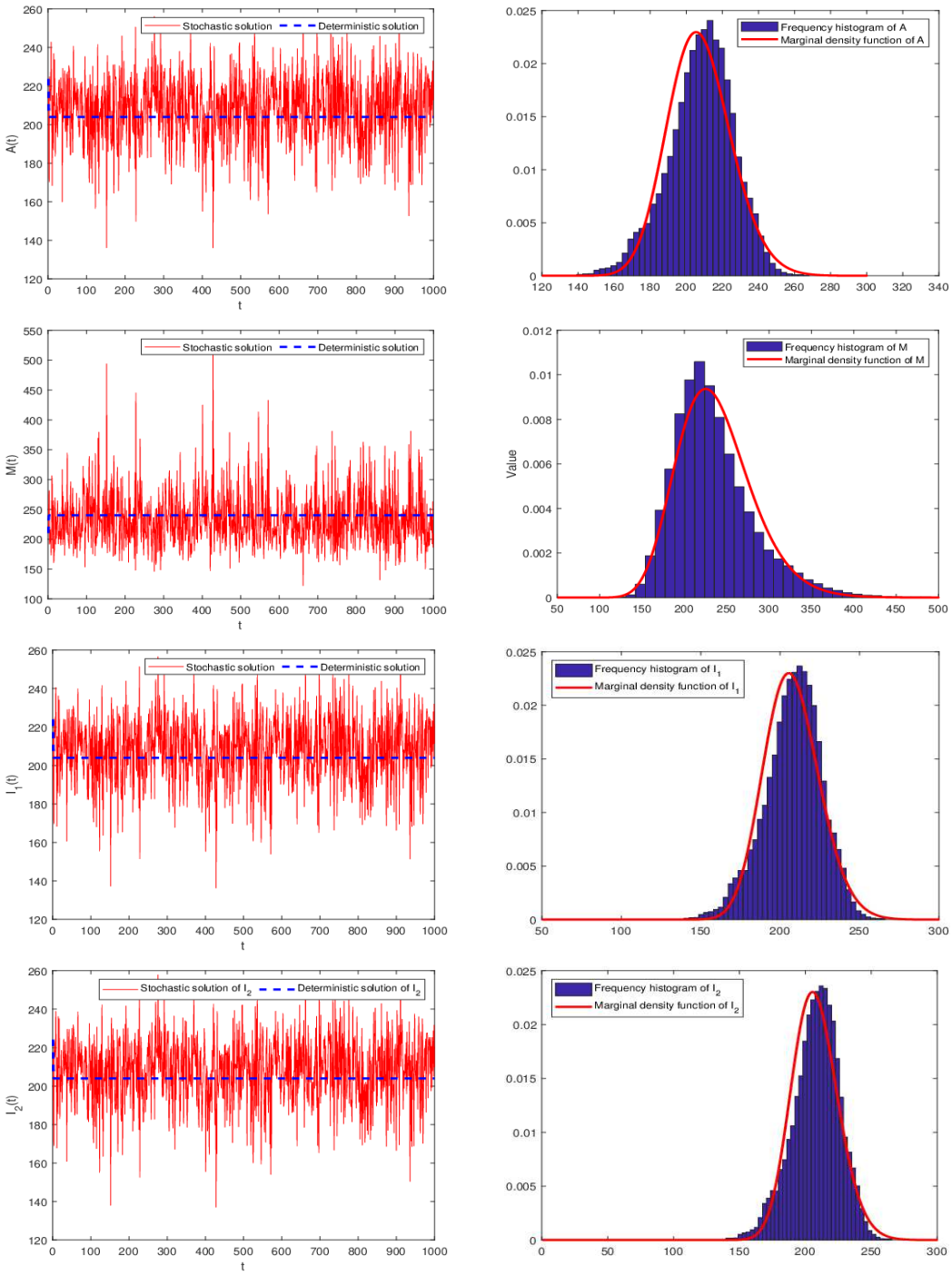

Figure 1: The left-hand column presents the sample path of $A(t), M(t), I_1(t)$ and $I_2(t)$ of model (2.1) with strong kernel and of its deterministic model (1.2) with strong kernel on $t \in [0,1000]$, respectively. The right-hand column shows the frequency histograms with 1000000 iteration points, and marginal density curves, respectively.

where

$$G=\left(\ln\frac{A}{239.70},\ln\frac{M}{166.95},\ln\frac{I_1}{239.70},\ln\frac{I_2}{239.70}\right).$$

From this, we can derive the following marginal density functions:

$$\Phi_\partial^*(A)=\frac{0.9044}{A}e^{-371.6002(\ln A-5.4794)^2},\quad \Phi_\partial^*(M)=\frac{0.3025}{M}e^{-0.8695(\ln M-5.1177)^2},$$

$$\Phi_\partial^*(I_1)=\frac{0.0065}{I_1}e^{-1857.4495(\ln I_1-5.4794)^2},\quad \Phi_\partial^*(I_2)=\frac{0.0103}{I_2}e^{-755.6252(\ln I_2-5.4794)^2}.$$

To illustrate Theorem 4.1 and to examine the local fitting effect of $\Phi^*(A,M,I_1,I_2)$, we plot the frequency histogram fitting curves of A,M,I_1 and I_2 at iteration points $n=1000000$. The marginal density functions of $\Phi_\partial^*(A),\Phi_\partial^*(M),\Phi_\partial^*(I_1)$ and $\Phi_\partial^*(I_2)$ closely align with the corresponding four fitting curves, as illustrated in Fig. 2.

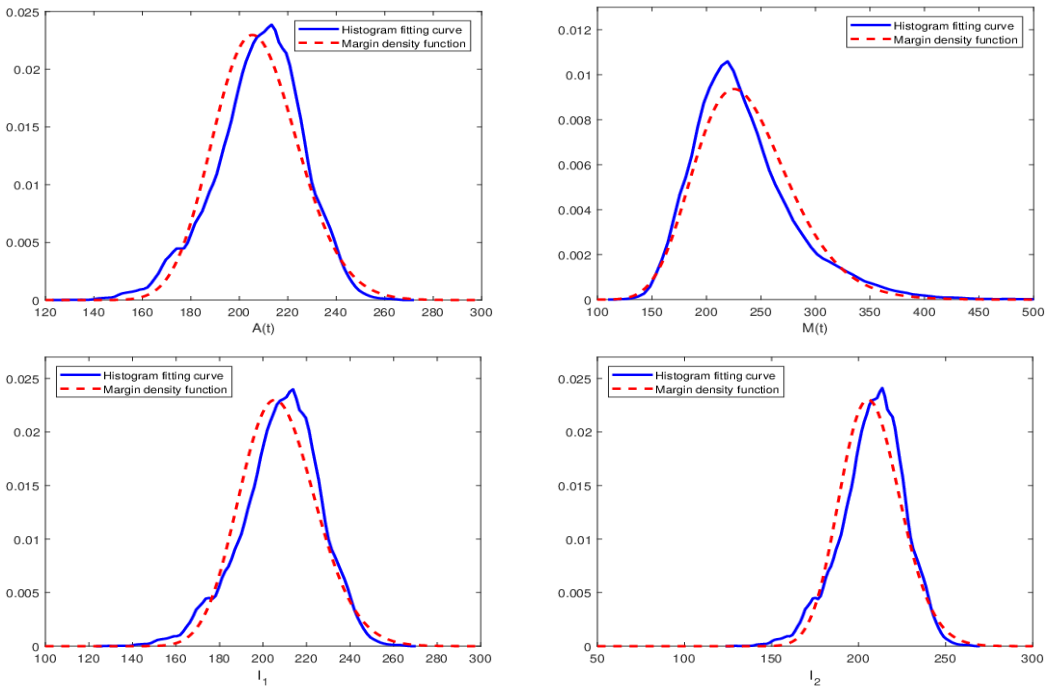

Figure 2: The blue line represents the frequency histogram fitting curve of A,M,I_1 and I_2, respectively. The red line denotes the corresponding marginal densities $\Phi_\partial^*(A),\Phi_\partial^*(M),\Phi_\partial^*(I_1)$ and $\Phi_\partial^*(I_2)$ of the approximate density function $\Phi^*(A,M,I_1,I_2)$.

6.2 Mussel extinction of system (2.1)

We select $\sigma_{11}=0.1,\sigma_{21}=4,\sigma_{22}=0.01$ in this subsection. By calculation, we obtain that $R_{03}=0.6667<1$. According to Theorem 5.1, the mussel species will undergo exponential decline with probability one, indicating that the mussel invasion has failed and the algae

will persist in the long term. Fig. 3 presents the corresponding computer simulations of the solution to system (2.1) with the strong kernel. Furthermore, to investigate the impact of delays on the rate at which mussels filter algae, we reduce T_e from 0.5 to 0.05 and 0.0025. In each case, the mussel invasion was unsuccessful, as illustrated in Fig. 4.

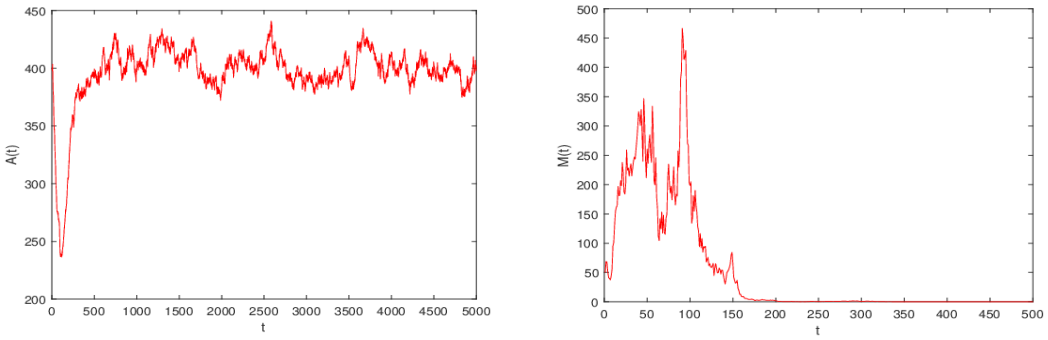

Figure 3: Computer simulations for A and M of model (2.1) with strong kernel and $\sigma_{21}=4$. Other parameters are the same as those in Fig. 1.

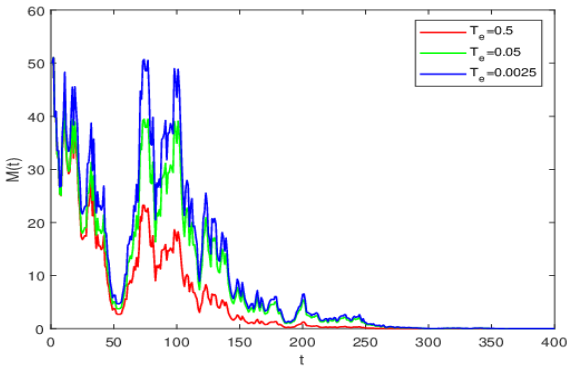

Figure 4: Computer simulations for mussel population $M(t)$ of model (2.1) with different mean time delays: $T_e=0.5$ (red line), $T_e=0.05$ (green line) and $T_e=0.0025$ (blue line). Other parameters are the same as those in Fig. 1.

6.3 Mean first passage time

The filter-feeding rate of invasive mussels directly influences their ability to establish themselves in a new environment. This sensitivity of the mussel filter-feeding rate to varying intensities of environmental disturbances necessitates an investigation into the switching time required for invasive mussels to transition from the initial state $(A(0),\ M(0), I_1(0), I_2(0))$ to the extinct state. Generally, the switching time is referred to as the first passage time (FPT), defined as the time taken for a random trajectory to reach a different regime for the first time [5].

The statistical average of the FPT is termed the mean first passage time (MFPT), which is one of the most effective methods for capturing the switching dynamics of mussel concentration. Following the approach outlined in [44], we present the MFPT of system (2.1) with the strong kernel, transitioning from the initial state to the mussel extinct state. The initial value is denoted as X_0, and we define the FPT as

$$\tau = \inf\{t : M(t) < 0.001\}.$$

Taking an average on the FPT generates the MFPT,

$$\text{MFPT} = \mathbb{E}[\tau].$$

Applying the Monte Carlo method for the numerical simulation, if $M(n\Delta t) < 0.001$, then $\tau = n\Delta t$. Let the number of simulation times $N = 1000000$, then

$$\text{MFPT} = \frac{\sum_{i=0}^{N} n_i \Delta t}{N}.$$

Fig. 5 shows the MFPT with c and σ_{21}.

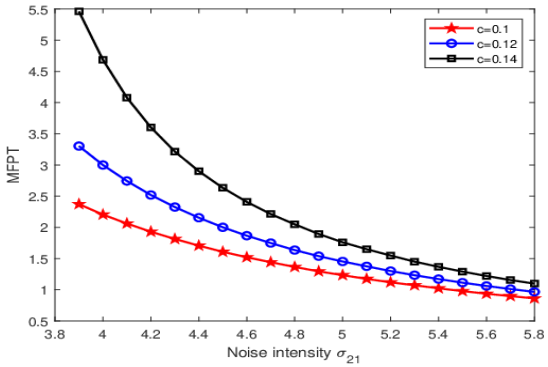

Figure 5: Mean first passage time of invasive mussels with the initial value $(A(0), M(0), I_1(0), I_2(0)) = (400,50,100,100)$. The other parameters are the same as those in Fig. 3.

6.4 Discussions

The filter-feeding behavior exhibited by invasive mussels plays a crucial role in their survival and success in invasion. Influenced by extrinsic factors such as manual removal and environmental fluctuations, the proposed model effectively incorporates the effects of intrinsic factors – particularly the filter-feeding rate – on the survivability of invasive mussels by integrating time delays. Using linear techniques, we first transform model (1.3) into an equivalent $(m+3)$-dimensional model (2.1). We then theoretically verify the existence and uniqueness of a global positive solution, thereby confirming the biological validity of the stochastic model. Subsequently, we establish sufficient conditions, $R_{01} > 1$, for the existence of an invariant probability measure, indicating that the invasive mussel population persists with probability one, signifying a successful mussel invasion. The in-

variant probability measure is a critical property, as it demonstrates that mussel invasions exhibit consistent statistical characteristics (such as mean and variance) over time.

Moreover, we define a quasi-endemic equilibrium X^* for model (4.2). A novel contribution of this paper is the theoretical derivation of an approximate expression (4.10) for the probability density function of the distribution $\omega(\cdot)$ around the equilibrium X^*. Numerical results indicate that, under certain conditions of small stochastic noise, the local approximate density function in (4.2) effectively fits the density function of the distribution (see Fig. 2).

Next, we establish the sufficient condition $R_{03} < 1$ for the exponential extinction of mussels, suggesting that noise can hinder the mussels' ability to successfully invade new waters (see Fig. 3). Additionally, simulations reveal that while random perturbations do not affect the stability of the equilibrium point, they do influence the rate at which mussels filter feed to acquire algae, ultimately impacting the extinction rate of mussels (see Fig. 4).

Finally, we quantify the impact of the filter-feeding rate c on the MFPT for invasive mussel biomass to transition from the initial state $M(0)$ to extinction. Numerical results demonstrate that, with a constant consumption rate c greater environmental noise accelerates the transition of invasive mussels from the initial state to extinction, indicating that environmental disturbances can more rapidly thwart successful mussel invasions. Furthermore, as illustrated in Fig. 5, under the same environmental noise conditions, a higher consumption rate slows the time required for invasive mussels to transition from the initial state to extinction.

In summary, this study effectively integrates internal factors influencing mussel survival, such as filter-feeding rates, with external factors, including environmental stochasticity and manual removal, within a dynamic framework that considers their interactions with algae, the primary food source. Although valuable insights have been obtained, there remain opportunities for further refinement. Future research should aim to comprehensively characterize the various life stages of mussels, including the suspension of larvae in the water column. It is crucial to consider the synergistic effects of invasive mussels across different life stages – specifically, the spatial propagation of larvae and the filter-feeding effects of adult mussels on algae. Additionally, examining the effects of bottom sediment in waters invaded by mussels presents a promising avenue for refining the current model and achieving a more thorough understanding of the dynamics associated with invasive mussels.

Appendix A. Some useful results

Throughout this paper, let $\{\Omega,\mathfrak{F},\{\mathfrak{F}_t\}_{t\geq 0},\mathbb{P}\}$ be a complete filtered probability space with a $\{\mathfrak{F}_t\}_{t\geq 0}$ satisfying the usual conditions (i.e. it is right continuous and increasing while $\mathfrak{F}_0$ contains all $\mathbb{P}$-null sets). Over this probability space, consider a ℓ-dimensional stochastic differential equation

$$\mathrm{d}X(t)=f\big(t,X(t)\big)\mathrm{d}t+\sum_{k=1}^{\ell}g_r\big(t,X(t)\big)\mathrm{d}B_r(t),\quad X(t)\in\mathbb{R}^{\ell} \tag{A.1}$$

with initial value $X_0\in\mathbb{R}^{\ell}$, where the vectors $f(t,x),g_1(t,x),\cdots,g_r(t,x)$ are continuous functions of (t,x). Subsequently, based on Khasminskii's ergodic theory [13], the existence of a corresponding stationary solution is addressed in the following lemma.

Lemma A.1 ([13]). *If the coefficients of* (A.1) *satisfy the following conditions:*

$$|f(t,x)-f(t,y)|+\sum_{r=1}^{\ell}|g_r(t,x)-g_r(t,y)|\leq \mathrm{Y}|x-y|, \tag{A.2}$$

$$|f(t,x)|+\sum_{r=1}^{\ell}|g_r(t,x)|\leq \mathrm{Y}(1+|x|), \tag{A.3}$$

where Y *is some constant. There exists a non-negative* C^2*-function* $V(x)$ *such that* $\mathcal{L}V\leq -1$ *outside of a certain compact set, where* $\mathcal{L}$ *denotes the differential operator as defined in* [22]. *Then the Markov process* $X(t)$ *of system* (A.1) *is ergodic and has a unique stationary distribution on* $\mathbb{R}^{\ell}$.

Below, we introduce the Routh-Hurwitz criteria and develop standard matrix theory relevant to solving Fokker-Planck equations.

Definition A.1. *The characteristic polynomial of the square matrix* $A_{\ell\times\ell}$ *is defined as*

$$\psi_A(\lambda)=\lambda^{\ell}+\sum_{i=1}^{\ell}a_i\lambda^{\ell-i},$$

then matrix A *has eigenvalues with all negative real components if and only if* $|H_\ell|>0$, *where* H_ℓ *is the* ℓ*-dimensional Hurwitz matrix defined by*

$$H_\ell=\begin{pmatrix} a_1 & a_3 & a_5 & \cdots & a_{2\ell-1}\\ 1 & a_2 & a_4 & \cdots & a_{2\ell-2}\\ 0 & a_1 & a_3 & \cdots & a_{2\ell-3}\\ 0 & 1 & a_2 & \cdots & a_{2\ell-4}\\ \vdots & \vdots & \vdots & \ddots & \vdots\\ 0 & 0 & 0 & \cdots & a_\ell \end{pmatrix}$$

with $a_j=0$ *if* $j>\ell$.

Lemma A.2. *For a real algebraic equation* $\Lambda^2+J\Sigma+\Sigma J^{\top}=0$, *where* $\Lambda=\mathrm{diag}(1,0,0,0)$ *and*

$$J=\begin{pmatrix} -r_1 & -r_2 & -r_3 & -r_4\\ 1 & 0 & 0 & 0\\ 0 & 1 & 0 & 0\\ 0 & 0 & 1 & 0 \end{pmatrix}.$$

If Σ is a four-dimensional symmetric matrix with $r_1>0, r_3>0, r_4>0$ and $r_1r_2r_3-r_3^2-r_1^2r_4>0$, then Σ is a positive definite matrix. Similarly, r_i $(i=1,2,3,4)$ are the coefficients of the characteristic polynomial $\psi_J(x)=x^4+r_1x^3+r_2x^2+r_3x+r_4$ of J.

Appendix B. Construction of four-dimensional standard R_4 matrix

Motivated by the work of [46], for the algebraic equation $\bar{\Lambda}^2+\bar{J}\bar{\Sigma}+\bar{\Sigma}\bar{J}=0$ with $\bar{\Lambda}=\mathrm{diag}(\delta,0,0,0)$, we present the developed theory for the four-dimensional standardized transformation matrices as follows:

$$\bar{J}=\begin{pmatrix} -a_{11} & 0 & 0 & -a_{12} \\ \alpha_1 & -\alpha_1 & 0 & 0 \\ 0 & \alpha_1 & -\alpha_1 & 0 \\ 0 & 0 & a_{24} & -a_{22} \end{pmatrix},$$

where $\alpha_1\neq 0$ and $a_{24}\neq 0$. According to the linear transformation of ordinary differential equations, we define a vector $X=(x_1,x_2,x_3,x_4)$ satisfying $\mathrm{d}X=\bar{J}X\mathrm{d}t$. In addition, we consider another vector $Y=(y_1,y_2,y_3,y_4)$ which satisfies

$$\begin{aligned} &y_4=x_4,\quad y_3=y_4^{'}=a_{24}x_3-a_{22}x_4,\quad y_2=y_3^{'}=a_{24}\alpha_1x_2-a_{24}(\alpha_1+a_{22})x_3+a_{22}^2x_4,\\ &y_1=y_2^{'}=a_{24}\alpha_1^2x_1-a_{24}\alpha_1(a_{22}+2\alpha_1)x_2+a_{24}\left(\alpha_1^2+a_{22}\alpha_1+a_{22}^2\right)x_3-a_{22}^3x_4. \end{aligned}$$

Thus, we obtain a standardized transformation matrix

$$P_1=\begin{pmatrix} a_{24}\alpha_1^2 & -a_{24}\alpha_1(a_{22}+2\alpha_1) & a_{24}\left(a_{22}^2+a_{22}\alpha_1+\alpha_1^2\right) & -a_{22}^3 \\ 0 & a_{24}\alpha_1 & -a_{24}(a_{22}+\alpha_1) & a_{22}^2 \\ 0 & 0 & a_{24} & -a_{22} \\ 0 & 0 & 0 & 1 \end{pmatrix}.$$

It is clear to see that $\mathrm{d}Y=P_1\mathrm{d}X=P_1\bar{J}X\mathrm{d}t=P_1\bar{J}P_1^{-1}Y\mathrm{d}t$, that is

$$\mathrm{d}Y=\begin{pmatrix} -q_1 & -q_2 & -q_3 & -q_4 \\ 1 & 0 & 0 & 0 \\ 0 & 1 & 0 & 0 \\ 0 & 0 & 1 & 0 \end{pmatrix}Y\mathrm{d}t,$$

where $\tilde{a}_{1i}$ $(i=1,\ldots,4)$ is the same as that in Theorem 4.1. Thus, we obtain the standard R_4 matrix M_1, which satisfies $M_1=P_1\bar{J}P_1^{-1}$.

Let $\rho_1=\alpha_1^2a_{24}\delta, \bar{\Sigma}_0=\rho_1^{-2}M_1\bar{\Sigma}M^{\top}$, the equation $\bar{\Lambda}^2+\bar{J}\bar{\Sigma}+\bar{\Sigma}\bar{J}=0$ can be equivalently rewritten as

$$\bar{\Lambda}_0^2+M_1\bar{\Sigma}_0+\bar{\Sigma}_0M_1^{\top}=0,$$

where $\bar{\Lambda}_0=\mathrm{diag}(1,0,0,0)$. Thus, the four-dimensional standardized transformation matrix of $\bar{J}$ is derived.

Acknowledgments

This research is supported by the National Natural Science Foundation of China (No. 12471465) and by the Natural Science Foundation of Shanghai (No. 23ZR1445100).

References

[1] C. H. Barbosa, C. M. Dias, D. H. Pastore, J. C. Silva, A. R. Costa, I. P. Santos, R. Z. Azevedo, R. M. Figueira, and H. F. Fortunato, *Analysis of a mathematical model for golden mussels infestation*, Ecol. Model., 486:110502, 2023.

[2] C. V. Baxter, K. D. Fausch, M. Murakami, and P. L. Chapman, *Fish invasion restructures stream and forest food webs by interrupting reciprocal prey subsidies*, Ecology, 85(10):2656–2663, 2004.

[3] K. A. Bruner, S. W. Fisher, and P. F. Landrum, *The role of the zebra mussel, Dreissena polymorpha, in contaminant cycling: II. Zebra mussel contaminant accumulation from algae and suspended particles, and transfer to the benthic invertebrate, Gammarus fasciatus*, J. Gt. Lakes Res., 20(4):735–750, 1994.

[4] R. A. Cangelosi, D. J. Wollkind, B. J. Kealy-Dichone, and I. Chaiya, *Nonlinear stability analyses of Turing patterns for a mussel-algae model*, J. Math. Biol., 70:1249–1294, 2015.

[5] J. Q. Duan, *An Introduction to Stochastic Dynamics*, in: Cambridge Texts in Applied Mathematics, Vol. 51, Cambridge University Press, 2015.

[6] A. Eleftheriou, *Methods for the Study of Marine Benthos*, John Wiley & Sons, 2013.

[7] C. Gardiner, *Handbook of Stochastic Methods: For Physics, Chemistry and the Natural sciences*, in: Springer Series in Synergetics, Springer, 1994.

[8] B. T. Han and D. Q. Jiang, *Threshold dynamics and probability density functions of a stochastic predator-prey model with general distributed delay*, Commun. Nonlinear Sci. Numer. Simul., 128:107596, 2024.

[9] S. Higgins and M. V. Zanden, *What a difference a species makes: A meta-analysis of dreissenid mussel impacts on freshwater ecosystems*, Ecol. Monogr., 80(2):179–196, 2010.

[10] D. J. Higham, *An algorithmic introduction to numerical simulation of stochastic differential equations*, SIAM Rev., 43(3):525–546, 2001.

[11] N. Ikeda and S. Watanabe, *Stochastic Differential Equations and Diffusion Processes*, Elsevier, 2014.

[12] C. B. Jørgensen, P. S. Larsen, and H. U. Riisgård, *Effects of temperature on the mussel pump*, Mar. Ecol. Prog. Ser., 64:89–97, 1990.

[13] R. Khasminskii, *Stochastic Stability of Differential Equations*, in: Stochastic Modelling and Applied Probability, Vol. 66, Springer Science & Business Media, 2011.

[14] P. Kishore, J. Hunter, C. Zeng, and P. C. Southgate, *The effects of different culture apparatuses and current velocities on byssus production by the black-lip pearl oyster, Pinctada margaritifera*, Aquaculture, 434:74–77, 2014.

[15] J. V. D. Koppel, M. Rietkerk, N. Dankers, and P. M. Herman, *Scale-dependent feedback and regular spatial patterns in young mussel beds*, Am. Nat., 165(3):E66–E77, 2005.

[16] J. Lei, B. S. Payne, and S. Y. Wang, *Filtration dynamics of the zebra mussel, Dreissena polymorpha*, Can. J. Fish. Aquat. Sci., 53(1):29–37, 1996.

[17] S. G. Li, Z. Q. Xia, Y. Y. Chen, Y. C. Gao, and A. B. Zhan, *Byssus structure and protein composition in the highly invasive fouling mussel Limnoperna fortunei*, Front. Physiol., 9:418, 2018.

[18] Q. X. Liu, A. Doelman, V. Rottschäfer, M. de Jager, P. M. Herman, M. Rietkerk, and J. V. D. Koppel, *Phase separation explains a new class of self-organized spatial patterns in ecological systems*, Proc. Natl. Acad. Sci. USA, 110(29):11905–11910, 2013.

[19] Q. X. Liu, P. M. Herman, W. M. Mooij, J. Huisman, M. Scheffer, H. Olff, and J. V. D. Koppel, *Pattern formation at multiple spatial scales drives the resilience of mussel bed ecosystems*, Nat. Commun., 5(1):5234, 2014.

[20] Q. Liu and D. Q. Jiang, *Periodic solution and stationary distribution of stochastic predator-prey models with higher-order perturbation*, J. Nonlinear Sci., 28:423–442, 2018.

[21] R. N. Mack, D. Simberloff, W. Mark Lonsdale, H. Evans, M. Clout, and F. A. Bazzaz, *Biotic invasions: Causes, epidemiology, global consequences, and control*, Ecol. Appl., 10(3):689–710, 2000.

[22] X. R. Mao, *Stochastic Differential Equations and Applications*, Horwood Publishing Limited, 1997.

[23] R. M. May, *Time-delay versus stability in population models with two and three trophic levels*, Ecology, 54(2):315–325, 1973.

[24] S. M. Melo-Merino, H. Reyes-Bonilla, and A. Lira-Noriega, *Ecological niche models and species distribution models in marine environments: A literature review and spatial analysis of evidence*, Ecol. Model., 415:108837, 2020.

[25] E. L. Mills, G. Rosenberg, A. P. Spidle, M. Ludyanskiy, Y. Pligin, and B. May, *A review of the biology and ecology of the quagga mussel (Dreissena bugensis), a second species of freshwater dreissenid introduced to North America*, Am. Zool., 36(3):271–286, 1996.

[26] R. Naddafi, P. Eklöv, and K. Pettersson, *Stoichiometric constraints do not limit successful invaders: Zebra mussels in Swedish lakes*, PLoS One, 4(4):e5345, 2009.

[27] D. H. Nguyen and G. Yin, *Coexistence and exclusion of stochastic competitive Lotka-Volterra models*, J. Differ. Equations, 262(3):1192–1225, 2017.

[28] M. J. O'Donnell, M. N. George, and E. Carrington, *Mussel byssus attachment weakened by ocean acidification*, Nat. Clim. Change, 3(6):587–590, 2013.

[29] H. Roozen, *An asymptotic solution to a two-dimensional exit problem arising in population dynamics*, SIAM J. Appl. Math., 49(6):1793–1810, 1989.

[30] S. G. Ruan, *Delay differential equations in single species dynamics*, in: Delay Differential Equations and Applications. NATO Science Series, Vol. 205, Springer, 477–517, 2006.

[31] M. Scheffer, S. H. Hosper, M. L. Meijer, B. Moss, and E. Jeppesen, *Alternative equilibria in shallow lakes*, Trends Ecol. Evol., 8(8):275–279, 1993.

[32] J. C. R. Silva, C. M. Dias, D. H. Pastore, A. R. C. Costa, and R. M. A. Figueira, *Population growth of the golden mussel (L. fortunei) in hydroelectric power plants: A study via mathematical and computational modeling*, Braz. J. Water Resour., 27:e3, 2022.

[33] A. V. Skorokhod, *Asymptotic Methods in the Theory of Stochastic Differential Equations*, in: Translations of Mathematical Monographs, Vol. 78, AMS, 2009.

[34] Y. L. Song, H. P. Jiang, Q. X. Liu, and Y. Yuan, *Spatiotemporal dynamics of the diffusive mussel-algae model near Turing-Hopf bifurcation*, SIAM J. Appl. Dyn. Syst., 16(4):2030–2062, 2017.

[35] R. Sousa, A. Novais, R. Costa, and D. L. Strayer, *Invasive bivalves in fresh waters: Impacts from individuals to ecosystems and possible control strategies*, Hydrobiologia, 735:233–251, 2014.

[36] X. Tian and C. Ren, *Linear equations, superposition principle and complex exponential notation*, Coll. Phys., 23:23–25, 2004.

[37] M. J. Vanni, *Invasive mussels regulate nutrient cycling in the largest freshwater ecosystem on Earth*, Proc. Natl. Acad. Sci. USA, 118(8):e2100275118, 2021.

[38] P. M. Vitousek, L. R. Walker, L. D. Whiteaker, D. Mueller-Dombois, and P. A. Matson, *Biolog-*

ical invasion by Myrica faya alters ecosystem development in Hawaii, Science, 238(4828):802–804, 1987.

[39] T. R. Whittier, P. L. Ringold, A. T. Herlihy, and S. M. Pierson, *A calcium-based invasion risk assessment for zebra and quagga mussels (Dreissena spp)*, Front. Ecol. Environ., 6(4):180–184, 2008.

[40] G. S. K. Wolkowicz, H. X. Xia, and S. G. Ruan, *Competition in the chemostat: A distributed delay model and its global asymptotic behavior*, SIAM J. Appl. Math., 57(5):1281–1310, 1997.

[41] G. S. K. Wolkowicz, H. X. Xia, and J. H. Wu, *Global dynamics of a chemostat competition model with distributed delay*, J. Math. Biol., 38:285–316, 1999.

[42] Y. Wu, S. M. Bartell, J. Orr, J. Ragland, and D. Anderson, *A risk-based decision model and risk assessment of invasive mussels*, Ecol. Complex., 7(2):243–255, 2010.

[43] Z. Xia, H. J. MacIsaac, R. E. Hecky, D. C. Depew, G. D. Haffner, and R. P. Weidman, *Multiple factors regulate filtration by invasive mussels: Implications for whole-lake ecosystems*, Sci. Total Environ., 765:144435, 2021.

[44] A. J. Yang, H. Wang, T. H. Zhang, and S. L. Yuan, *Stochastic switches of eutrophication and oligotrophication: Modeling extreme weather via non-Gaussian Lévy noise*, Chaos, 32(4):043116, 2022.

[45] X. W. Yu and S. L. Yuan, *Asymptotic properties of a stochastic chemostat model with two distributed delays and nonlinear perturbation*, Discrete Contin. Dyn. Syst. Ser. B, 25(7):2373–2390, 2020.

[46] B. Q. Zhou, H. Wang, T. X. Wang, and D. Q. Jiang, *Stochastic generalized Kolmogorov systems with small diffusion: I. Explicit approximations for invariant probability density function*, J. Differ. Equations, 382:141–210, 2024.